Kinetics driving thin-film deposition in dielectric barrier discharges using a direct liquid injector operated in a pulsed regime

L. Cacot, G. Carnide, Myrtil L Kahn, Richard Clegereaux, Nicolas Naude, Luc Stafford

Kinetics driving thin-film deposition in dielectric barrier discharges using a direct liquid injector operated in a pulsed regime

L. Cacot [1,3], G. Carnide [1,2], M. L. Kahn [2], R. Clergereaux[1],

N. Naudé[1*] and L. Stafford[3†]

[1]Département de physique, Université de Montréal, Montréal, Québec, Canada

[2]LAPLACE, Université de Toulouse, CNRS, INPT, UPS, Toulouse, France

[3]LCC, CNRS (UPR 8241), Université de Toulouse, Toulouse, France

Abstract

This work investigates the effects of process parameters on thin-film deposition by Direct Liquid Injection in a low-frequency Dielectric Barrier Discharge (DBD). The precursor, hexamethyldisiloxane (HMDSO), is introduced as micrometer-size liquid droplets with nitrogen carrier gas in a pulsed mode and the discharge is produced at atmospheric pressure in a pulsed regime. No significant deposit is observed during plasma-off time and outside the discharge region. Despite the pulsed injection, this reveals that the precursor content in the plasma zone remains constant over much longer time scales and that thin-film deposition results from droplets charging and their transport towards the dielectrics by the low-frequency electric field. Over the range of experimental conditions investigated, it is

* Electronic mail: nicolas.naude@laplace.univ-tlse.fr

† Electronic mail: luc.stafford@umontreal.ca

found that pulsed, aerosol-assisted plasma deposition is limited by the amount of energy provided to precursor droplets, and not by precursor insufficiency.

Keywords: Dielectric Barrier Discharge, Atmospheric Pressure Plasma Processes, Pulsed Direct Liquid Injection, Aerosol-Assisted Plasma Deposition, Organosilicon Coatings.

1. Introduction

Atmospheric-pressure plasmas operated in reactive gas mixtures are widely used for (multi)functional thin-film deposition. Among them, Dielectric Barrier Discharges (DBD), one of the most well-developed non-equilibrium plasmas, are frequently used to deposit thins films on large area surfaces [1,2]. Considering their broad range of applications, including anti-fogging capacity, corrosion protection ability, biocompatibility, moisture barrier and water-repellent properties [3–13], organosilicon thin films have been extensively researched, and the parameters controlling their deposition kinetics, structure, and morphology have been widely investigated. Based on the available literature, the so-called Yasuda's parameter, a parameter equivalent to the ratio of discharge power to precursor flow rate (W/F), is an important factor affecting plasma-deposited thin films [14]. *Park et al.* [15] reported that this parameter influences the chemical structure, density, and yield of the material deposited by plasma polymerization of hexamethyldisilazane using a radio frequency capacitive discharge. Similarly, *Petersen et al.* [16] reported that at low W/F, plasma-assisted polymerization of hexamethyldisiloxane (HMDSO) is dominated by oligomerization, leading to polydimethylsiloxane thin films, whereas at high W/F, cross-linked SiO_x thin films are formed. *Bardon et al.* [17] also assessed the effects of plasma power and precursor flow rate on acrylate thin-film deposition by semi-dynamic DBD operated in helium with 1,6-hexanediol dimethacrylate precursor. Their results indicate that these parameters have a strong influence on the energy supplied to precursor molecules, and thus on the plasma-assisted precursor conversion rate.

In addition to Yasuda's parameter, the plasma deposition kinetics and precursor polymerization dynamics depend on the plasma power injection controlled, for example, by the plasma-on time (duty cycle) [18–20]. In such pulsed plasma conditions, *Manakhov et al.*[19] proposed that plasma-assisted deposition occurs only during plasma-on time, whereas free radical polymerization occurs during plasma-off time. The studies conducted on thin-film deposition by plasma polymerization at atmospheric pressure further show that the morphology of the deposited material depends on the nature and flow of the precursor, which is usually introduced into the plasma chamber either directly as a gas (for example, silane) or as a vapor from the liquid phase through an atomizing system (for example, HMDSO) [21–25]. In a study conducted on the deposition and polymerization of HMDSO by corona discharge, *O'Neil et al.* [26] showed that the surface morphology of the deposited material changes upon increasing the flow of the injected HMDSO precursor. The authors concluded that at low monomer flow rate, the precursor is fully vaporized, and deposition is due to the plasma polymerization of the gas-phase monomer. Meanwhile, at high flow rate, the precursor is not fully vaporized, and liquid droplets are introduced into the plasma chamber in the form of aerosols. Hence, droplets can interact with the plasma and contribute to the thin-film deposition process. The morphology of the organosilicon coatings deposited at high flow rate in the so-called misty plasma (combination of liquid, gas, and plasma states [27]) is different from the one achieved at low flow rate in a purely gas-phase plasma process. Despite the available studies, the effect of liquid droplets on plasma-assisted thin-film deposition at atmospheric pressure remains poorly understood due to the complexity of biphasic liquid-plasma interactions [28]. A better understanding of such features could bring new opportunities for material processing.

In this study, the effects of process parameters, namely, duty cycle, delay between precursor injection and discharge ignition, and the amount of injected HMDSO microdroplets on the plasma-assisted deposition of organosilicon thin films in low-frequency Townsend DBDs operated in nitrogen are assessed. In contrast to other studies based on aerosols and atmospheric-pressure plasmas reported in literature, direct-liquid injection and the discharge are both pulsed. This approach offers a wide parameter space for fundamental studies of misty plasmas at atmospheric pressure applied to thin-film deposition. Selected experiments are also done by varying the continuous flow of the N_2 gas used to carry along the discharge cell the precursor droplets injected and to underline the contributions of transport phenomena. Based on this complete set of data, the influence of the energy injected in the plasma per precursor molecule is explored and the predominant role of plasma-droplet interactions is highlighted.

2. Experimental setup and diagnostics

The experimental setup used in this study has been described previously [29–31]. It consists of a metallic chamber containing two horizontally mounted alumina plates coated with conductive silver paste to serve as plasma electrodes (3 cm × 6 cm). A silicon wafer substrate (4 cm × 7 cm) was fixed on the bottom alumina plate with Kapton tape, and two glass spacers were placed on top of the silicon substrate to keep the gas gap distance at 1 mm. In all experiments, the chamber was first filled with a continuous flow of N_2 gas (Alphagaz 1, Air Liquide) at atmospheric pressure. In this system, gas injection occurs through a diffuser located at the entrance of the plane-to-plane DBD cell, and a self-

regulating valve located between the outlet of the plasma chamber and the vacuum pump is used to maintain the pressure at 750 Torr. Here, the diffuser and glass spacers ensure a longitudinal flow of the carrier gas and precursor through the DBD cell between the two alumina plates. DBD was ignited between the two metallic electrodes by applying a 1 kHz, 13 $kV_{peak\ to\ peak}$ sinusoidal signal that is generated using a Tektronix AFG3021C power supply connected to a linear power amplifier whose output is linked to the primary winding of a step-up transformer. A high-voltage probe (TektronixP6015A) connected between the high-voltage electrode (top electrode) and ground was used to measure the applied voltage. The flowing current and charge were deduced from the voltage values measured across a 100 Ω shunt resistor and a 220 nF capacitor, respectively; both were placed in parallel between the low-voltage electrode (bottom electrode) and ground. Meanwhile, the power injected into the DBD was calculated from Lissajous plots, based on the electrical signals acquired using an oscilloscope (TELEDYNE Lecroy HD06104A) and the approach described in [32–34].

The liquid HMDSO precursor (SigmaAldrich) along with a nitrogen carrier gas was injected into the discharge using a commercialized, two-stage, direct-liquid-injection system purchased from Kemstream. More specifically, the liquid contained in the precursor chamber (first stage) is injected in a pulsed mode in the mixing chamber of the device (second stage) filled with N_2 (Alphagaz 1, Air Liquide). The content of the mixing chamber (HMDSO precursor droplets and nitrogen carrier gas) is then injected in pulsed mode through the diffuser in the plasma chamber. Injection, i.e. the quantity of liquid and gas injected in the DBD was controlled by the frequency and duration of the pulses. In this

work, only the duration of the pulsed liquid injection (from stage 1 to stage 2) was varied between 2 (lower limit recommended by the manufacturer is 1.5 ms) and 6 ms; the pulse duration of precursor droplets and carrier gas was kept constant to 10 ms. As for the pulse repetition frequency, it was fixed to 0.1 Hz; hence, over the range of experimental conditions investigated, the discharge "sees" a new pulse every 10 s. In some cases, a continuous nitrogen carrier gas flow (between 0.07 and 1.4 $L.min^{-1}$), in addition to the pulsed HMDSO aerosol in nitrogen, was applied while maintaining atmospheric-pressure conditions. Such flow was used to examine the role of continuous precursor transport (and thus of the precursor residence time) across the inter-dielectric space.

To characterize the aerosol, the spray was illuminated with a blue light and observed at 45° using a FastCAM camera (APX RS Photron, 1500 fps). The aerosol was analyzed by post processing the recorded images with a MATLAB program to assess the time evolution of the light intensity scattered by liquid microdroplets. As an example, images of an aerosol of HMDSO in nitrogen produced with a pulsed liquid injection of 5 ms under atmospheric pressure conditions is reported in Figure 1a along the pulse injection period. As can be seen, this aerosol is composed of microdroplets that expand at the outlet of the injector. Over the range of experimental conditions investigated, the expansion rate along the longitudinal axis is about 5 $m.s^{-1}$. In addition, the variation of the total light scattering (integrated over the whole images of Figure 1a) was calculated over time and plotted in Figure 1b. Microdroplets are observed for 10 ms after the liquid is first detected, which confirms that the entire process of liquid injection into the DBD reactor occurs within the

opening time of the second stage of the direct-liquid injection device, with no significant injection afterwards.

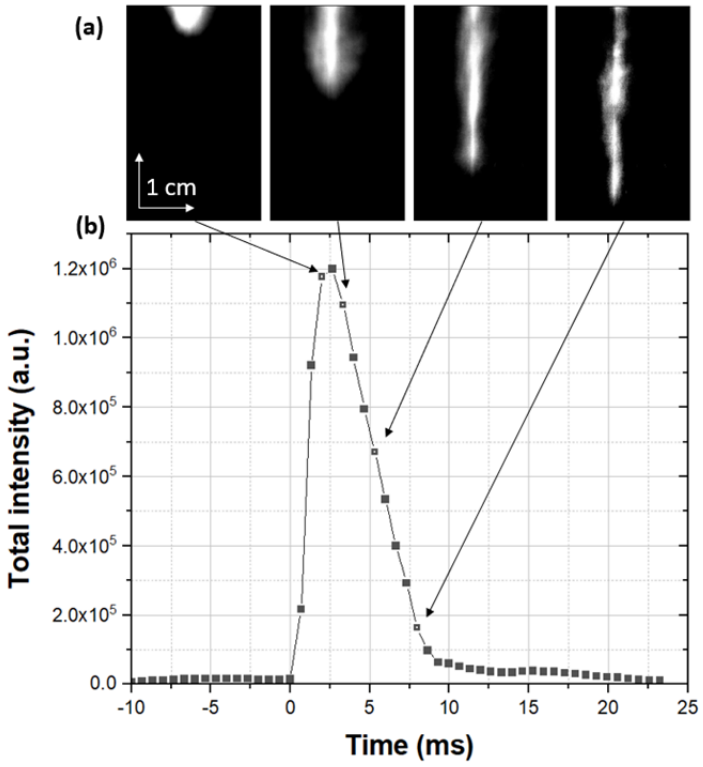

Figure 1: a) Fast camera images of the liquid precursor recorded at different times during the injection process. Of note, on each image, even if the maximum intensity decreases with time, the contrast was adjusted for aerosol visualization. b) Variation of the total light intensity scattered by liquid droplet as a function of time for 10 ms injection.

After plasma deposition, the silicon substrate was removed for thin-film thickness measurements. However, the plasma-deposited layers are soft and thus not easily measurable by profilometry. In addition, the composition and structure of the film are unknown to use a reliable spectroscopic ellipsometry model. Therefore, they were analyzed by Fourier Transform InfraRed (FTIR) in a transmission mode (Bruker). Of note, FTIR

spectra emphasize the typical bands reported in the literature of plasma-polymerized HMDSO with the main feature of Si–O–Si (1200–1000 cm^{-1}) bands [35–37]. Hence, considering Beer-Lambert law, FTIR is used to extract a relative thickness of the deposited thin film (in arbitrary unit) by integrating the area of the Si-O-Si absorption band.

3. Dielectric barrier discharge with direct liquid injection

The electrical characteristics (voltage, current, and charge) of nitrogen discharge with and without direct liquid injection are presented in Figure 2. As shown in Figure 2a, the electrical characteristics of the DBD generated with pulsed flow of N_2, in the absence of liquid HMDSO precursor, are representative of a homogeneous Townsend discharge [38]. Of note, depending on the experimental conditions, pulsed nitrogen gas injection in a Townsend discharge operated with a continuous nitrogen gas flow can destabilize the discharge [39]. Such effect is not linked to the sharp and narrow temporal gas velocity profiles, but rather to gas recirculations in presence of singular head losses. In a previous study [39], it was shown that these flow perturbations arising from irregularities from the inlet pipe to the gas mixing chamber and then to the DBD cell combined with impurities outgassing from the walls introduce significant changes in the neutral gas composition. In particular, the release of oxygen impurities with abnormal concentrations over time scales much longer than the pulse duration was shown to plays a vital role on the Townsend discharges' physics and characteristics. Here, to prevent gas recirculations and changes in the neutral gas composition, the gas and precursor inlet line were simplified to minimize

singular head losses. Consequently, identical current-voltage characteristics are recorded with continuous N_2 flow and pulsed N_2 gas injections.

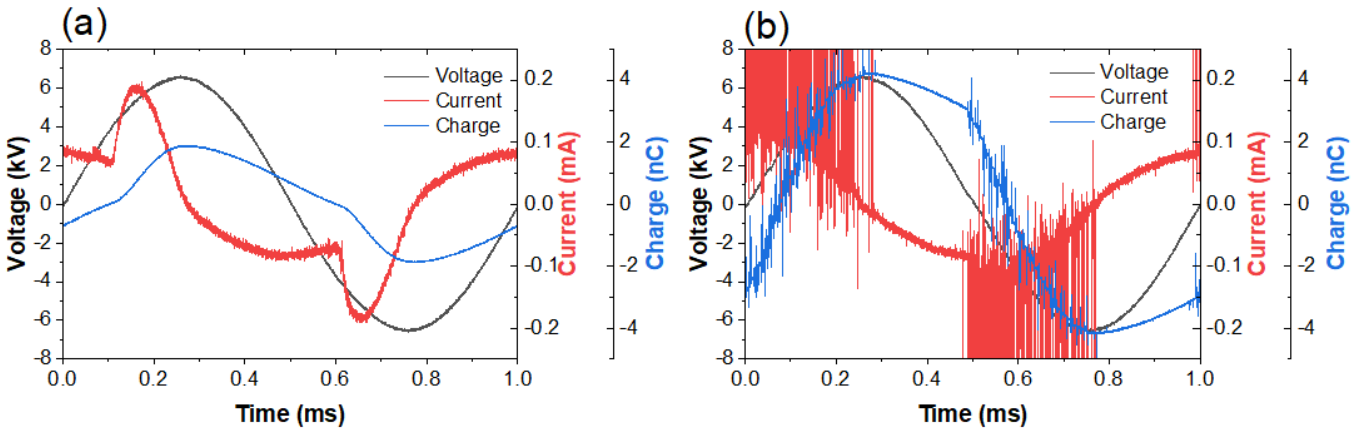

Figure 2: Applied voltage, current, and charge profiles recorded with pulsed N_2 flow (a) without and (b) with direct liquid HMDSO injection at 10 ms pulse duration and 0.1 Hz pulse frequency.

In the presence of a pulsed aerosol of HMDSO with nitrogen carrier gas, sudden current increase (shown by a saturation of the input channel of the oscilloscope) and increased charge values are detected (Figure 2b). This confirms that micro-discharges appear, and that the discharge transits from homogeneous to filamentary regime following direct injection of micrometer droplets [1,40]. Such features most likely arise due to the loss of long-lived metastable $N_2(A)$ states that are involved in the production of seed electrons by secondary electron emission [38], but also by associative ionization between excited nitrogen atoms and atomic oxygen [41,42].

4. Interaction between Townsend discharge and injected liquid

Figure 3 presents the spatial distribution of the organosilicon deposit collected after 2 min. of plasma discharge exposure for a 10 ms direct liquid injection duration and a 0.1 Hz liquid injection frequency. Considering the scheme of the deposition process, the deposit is observed only where the discharge occurs, i.e., between the two metallic electrodes that do not cover the whole surface of the two alumina plates. Pre- and post-discharge deposits are not visible to the naked eye. To confirm this observation, FTIR spectra of the substrate surface were recorded at five different positions along the gas flow lines. The graph in Figure 3 presents the spatial variation of the film relative thickness: it is higher between the electrodes, without deposition before and after the electrode area. Polymerization and deposition thus occur only in the presence of plasma. To corroborate this hypothesis, the same experiment was carried out at an applied voltage lower than the breakdown voltage. No deposition was observed, even if an electric field is present. This indicates that deposition results from plasma-droplet interactions.

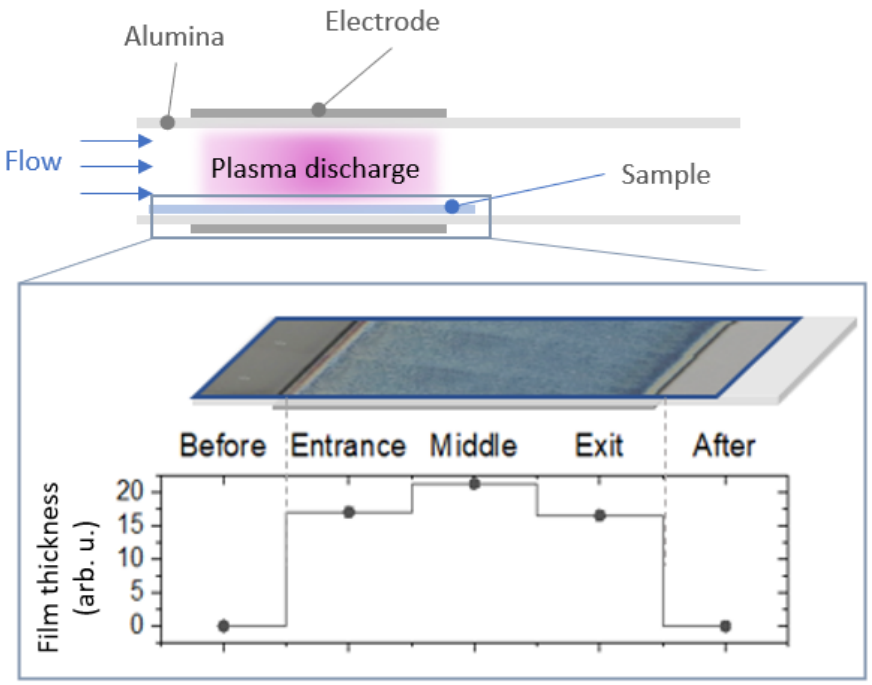

Figure 3: Scheme of the deposition process and spatial distribution of the organosilicon deposit. The results for the film thickness are obtained from the Si-O-Si band area recorded by FTIR analysis. As a rough estimate, a film thickness of about 20 arb. unit throughout this work corresponds to about 1 µm.

5. Thin-film deposition with direct liquid injection

5.1. Influence of plasma-on time

To understand the kinetics driving organosilicon thin film deposition with direct liquid injection, the discharge was pulsed in synchronization with each pulsed, 10 ms, 0.1 Hz injection of liquid. In the first set of experiments, the plasma-on time during which a voltage is applied between the two electrodes of the DBD cell was varied between 10 ms (during pulsed liquid injection with no time delay) and 10 s (referring to a continuous plasma) (Figure 4a). The material deposited on the substrate under different conditions for

a total process duration of 4 min. (24 pulses of HMDSO) was analyzed by FTIR, and the variation of the film thickness was extracted and plotted as a function of plasma-on time. In Figure 4b, the result for each condition corresponds to an average over all positions along the gas flow lines, and the error boxes represents the inhomogeneity of the film. Each experiment were repeated several times and standard deviation were low compared to thickness variations along the gas flow lines. As can be seen, the thickness of the deposited film linearly increases with plasma-on time up to 10 s. Hence, enhanced deposition rates over the total process duration of 4 min. are observed at longer plasma-on times, even though liquid injection occurs for only 10 ms. From this set of data, it seems that the amount of liquid injected within 10 ms interacts with the plasma for at least 10 s, and that the precursor remain confined in the plasma zone between the two electrodes over this whole timescale. Such conclusion reveals that the precursor is charged upon exposure to charged species as expected for micrometer droplets [43,44] and that thin-film deposition results from the transport of charged droplets towards the dielectrics by the low-frequency electric field. In such conditions, charged droplets in the misty plasma [27] behave as charged solid particles in a dusty plasma [27,45].

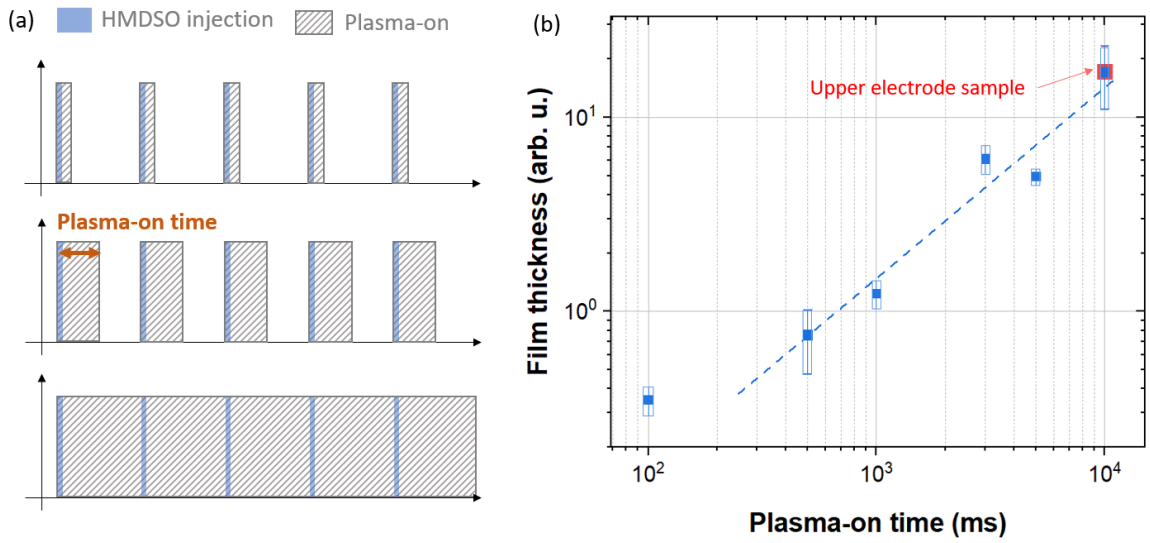

Figure 4: a) Schematics of the plasma-on time with respect to the pulsed HMDSO injection. The plasma-on time rises from the top to the bottom. b) Variation of the film thickness for a total process time of 4 min. (linked to the deposition rate) as a function of plasma-on time. Pulsed injection time of 10 ms, pulsed injection frequency of 0.1 Hz. Here, 10 s corresponds to a continuous plasma deposition. All measurements were recorded on a sample placed on the bottom dielectric, except for one condition highlighted in red as "Upper dielectric sample" which completely overlap the one obtained for the same treatment on the bottom electrode.

Knowing that the injected droplets can be deposited on both dielectrics, the top as well as the bottom one, an experiment was conducted to ensure that the material on the bottom dielectric is fully attributed to plasma processing and does not form over time due to other mechanisms such as gravity. In this experiment, the substrate was placed on the top dielectric, and the thickness of the film deposited on this substrate after 4 min. of continuous plasma processing (plasma-on time = 10 s) was measured (red square symbol in Figure 4b). Taking the error margins into account, the deposited film has the same thickness (and thus the same deposition rate) as the one deposited on the bottom dielectric under the same conditions. This indicates that the top dielectric is not a source of precursor

and therefore of plasma deposition. It further underlines that the low-frequency electrostatic force induces a motion of charged droplets towards both the top and bottom dielectrics and play a very important role in aerosol-assisted plasma deposition with respect to other ones such as gravitational, thermophoresis, and dielectrophoresis forces [45]. Notably, the film thickness measured at very short plasma-on times seems higher than the linearity line seen at longer times. However, recall that the films deposited at short plasma-on times are quite thin, and so, their measured thickness is largely uncertain. At plasma-on times greater than 500 ms, the ratio of film thickness to plasma-on time is constant. This confirms that the precursor is always present in the gas gap, even at liquid injection pulse durations as low as 10 ms.

5.2. Influence of the delay between liquid injection and discharge ignition

According to previous studies, thin-film deposition in pulsed plasmas can also occur during plasma-off time [19,20,46]. Herein, the impact of plasma-off time was assessed by varying the delay period between liquid injection and discharge ignition (Figure 5a). The plasma-on time was fixed at 500 ms and the delay time was varied from 0 to 5 s (a half time of the injection period). As shown in Figure 5b, the film thicknesses at 0, 100, 500, 1000, and 5000 ms delay times for a total process time of 4 min. are in the same range. This means that the deposition rate is independent of the delay time. Hence, the quantity of precursor does not change during the period between two pulses (i.e., 10 s for a liquid injection frequency of 0.1 Hz). Based on these results, the deposition occurring during

plasma-off time seems negligible compared to the one achieved during plasma-on time. This last observation further confirms a strong interaction between the injected droplets and the plasma. Upon plasma exposure, HMDSO droplets are charged such that they can become confined in the gas gap by the low-frequency electric field. The latter is also responsible for their transport towards the dielectric allowing the thin-film deposition. In line with this result, the transport of the droplets and their residence time in the inter-dielectric space can play a critical role in the deposition process. It is therefore proposed in the next section to analyse plasma assisted deposition in the presence of a continuous carrier gas flow of nitrogen, in addition to the pulsed HMDSO aerosol in nitrogen.

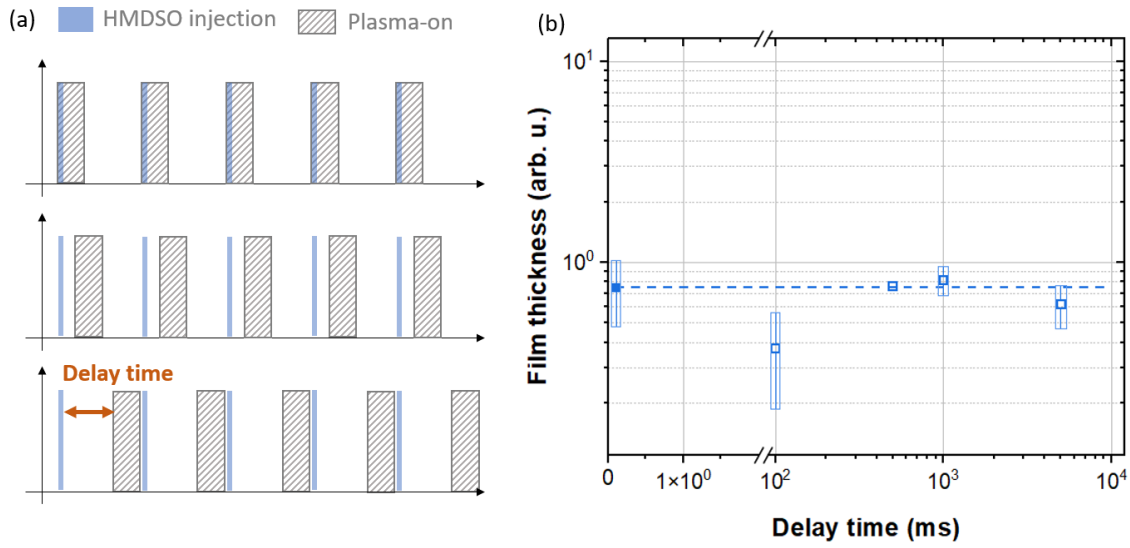

Figure 5: a) Schematics of the delay time with respect to the pulsed HMDSO injection. The delay time rises from the top to the bottom. b) Variation of the film thickness for a total process time of 4 min. (linked to the deposition rate)) as a function of delay time between liquid injection and discharge ignition. Pulsed injection time of 10 ms, pulsed injection frequency of 0.1 Hz, plasma-on time is fixed at 500 ms.

5.3. Influence of a continuous nitrogen gas flow

Most plasma processing studies involving continuous vapors or aerosols injection make use of a continuous carrier gas flow to transport the precursor towards the discharge zone. Modification of this flow rate induces variations in the residence time of the precursor because of drag forces between carrier gas and precursor droplets, thereby affecting the thickness of the plasma-deposited film. The film thicknesses for a total process duration of 4 min. are determined and reported on Figure 6a over the range of carrier gas flow of 0–2 L.min^{-1}. Clearly, the film thickness, and thus the film deposition rate significantly decreases with increasing rate of continuous gas flow. This can readily be explained by a lower residence time of HMDSO droplets in the plasma.

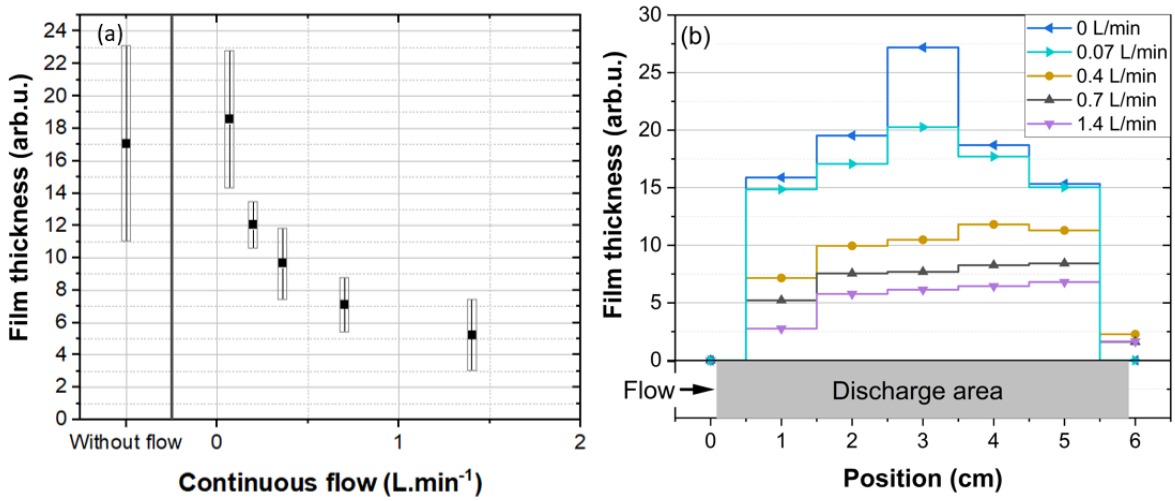

Figure 6: (a) Variation of the film thickness for a total process time of 4 min. (linked to the deposition rate) as a function of continuous N_2 gas flow rate. (b) Spatial deposition profiles along the gas flow lines recorded at different continuous flow rates. Pulsed injection time of 10 ms, pulsed injection frequency of 0.1 Hz, plasma-on time is fixed at 500 ms.

To further assess the role of carrier gas, coatings were analysed at seven different positions along the gas flow, under varying conditions of continuous N_2 flow rate. As shown in Figure 6b, when the flow rate of N_2 is lower than 0.1 L.min^{-1}, maximum deposition occurs at the centre of the substrate. As the flow rate is increased beyond 0.1 L.min^{-1} (up to ~2 L.min^{-1}), the maximum thickness of the deposited film decreases and moves closer to the outlet [47]. Notably, for this range of continuous gas flow, a small deposit is observed after the discharge compared to the absence of post discharge deposition without a continuous carrier gas. This result is consistent with the results reported by *Sarra-Bournet et al.* [48] which observe the appearance of a post discharge deposit by increasing the continuous flow in classical vapor-assisted plasma deposition conditions. Overall, these results indicate that the force on droplets linked to the presence of a nitrogen flow rate in the L.min^{-1} range can compete with the electrostatic force on charged droplets leading to thin-film deposition on the substrate surface. This explains the displacement of the deposit towards the exit at higher continuous N_2 gas flow rates. In addition, when the continuous flow rate increases, the residence time of the species in the inter-dielectric space decreases, and interactions between the plasma and the droplets are restricted, resulting in the deposition of thinner films.

In line with these findings, it can be proposed that thin-film deposition with direct-liquid injection in a DBD results from the mechanisms illustrated in Figure 7. Upon exposure to the low-frequency DBD, HMDSO droplets are rapidly charged. Considering average ion and electron number densities of ~10^{12} cm^{-3} in filamentary discharges operated in nitrogen [1] and assuming that the droplet charging time is given by the inverse of the

ion plasma frequency [49], charging of HMDSO droplets most likely occurs within ~5 ns. Hence, droplets become charged over times much shorter than (i) the time scales of microdischarges (~100 ns) in filamentary DBDs [34], (ii) the period of the applied electric field (1 ms at 1 kHz), and (iii) the gas residence times linked to pulsed (~3 ms) and continuous gas flows (~150 ms at 0.7 L/min).

Once charged, without continuous nitrogen gas flow, it was highlighted that the electrostatic force controls the droplet motion and thus the thin-film deposition over both top and bottom dielectrics. For a steady-state charge of ~10^4 electrons per 10 μm HMDSO droplet (and thus a mass-to-charge ratio ~10^2 kg/C) [44,50], the amplitude of oscillations of charged droplets in a 7.5 kV.mm^{-1} electric field at 1 kHz is comparable to the gas gap (~1 mm). This indicates that the collection of HMDSO droplets on the dielectrics leading to organosilicon thin-film deposition strongly depends on their size: droplets much smaller than 10 μm are easily collected within half-period of the applied electric field whereas droplets much larger than 10 μm remain trapped over multiple low-frequency cycles until they become pushed out of the DBD cell by the carrier gas. As the flow of continuous nitrogen gas increases, the contribution of the neutral drag force increases such that the transport of droplets along the gas flow lines becomes more important. For example, the ratio of neutral drag-to-Coulomb force amplitude on 10 μm HMDSO droplets with ~10^4 electrons is 1% at 0.07 L.min^{-1} and 17% at 1.4 L.min^{-1}.

In the collection criterion discussed above, HMDSO droplets immersed in the filamentary DBD were assumed to acquire a charge uniformly distributed over the whole

surface (see Figure 7). However, over the range of experimental conditions investigated, the Debye length in microdischarges is comparable to the droplet size. Thus, spatially inhomogeneous charging of HMDSO droplets can modify the balance between the inward surface tension of the liquid and the outward electrostatic and liquid pressure forces. This can cause the droplet to become unstable and undergo Coulomb fission [44,51], before reaching the so-called Rayleigh condition [52]. The result is the formation of smaller progeny droplets from unstable parent droplets. Because of the high amplitude of oscillations of progeny HMDSO droplets, they can more easily be collected on the substrate following their interaction with the low-frequency electric field. Hence, thin-film deposition using direct-liquid injection of HMDSO in the filamentary DBD may become linked to the amount of energy provided to precursor droplets for charging, electrostatic deformation, and fission; this aspect is examined in more details in the next section. Of note, as highlighted by *Coppins* [27], the time scales for droplet electrostatic deformation in misty plasma processes are usually much shorter than the one for droplet evaporation, both in and out of the plasma. Thus, for the Coulomb fission phenomenon of interest here, evaporation kinetics can be neglected.

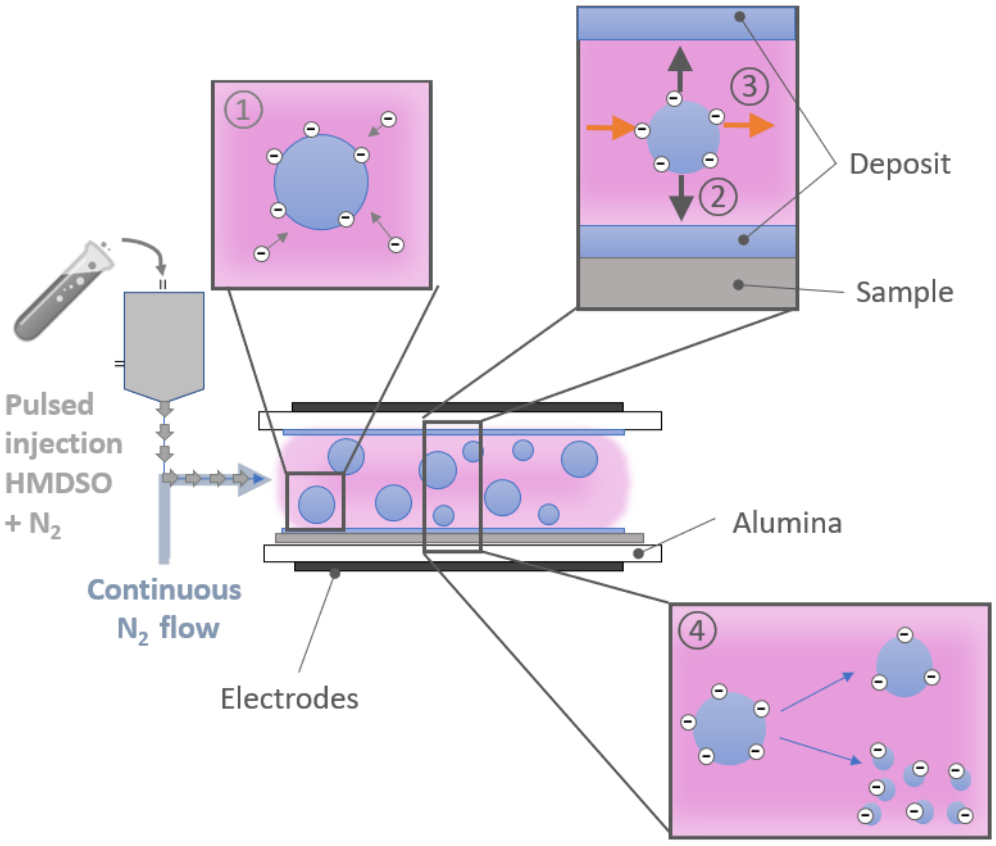

Figure 7:Scheme of the different mechanisms involved in thin-film deposition of organosilicon coatings by pulsed injection of HMDSO droplets into a DBD. Mechanisms include (1) droplet charging, (2) Coulomb and (3) Neutral drag forces on droplets, and (4) Electrostatic deformation leading to Coulomb fission.

5.4. Influence of the energy injected into the discharge

It is well-established that the Yasuda parameter relating plasma power to precursor flow rate is one of the most important factors affecting the plasma-precursor interaction and thus plasma deposition and polymerization kinetics. These studies make use of a continuous gas flow to transport the precursor vapor into the plasma. Considering that in some experiments conducted herein no continuous gas flow was used, we interpret the Yasuda parameter as the ratio of power injected into the DBD to precursor residence time.

In such case, the energy parameter can be defined as follow (also called by some authors Specific Energy Input (SEI) [53]):

$$E = P \times t_{residence} \times Duty\ Cycle \quad (1)$$

where P is the power determined from electrical analysis of the DBD, $t_{residence}$ is the average time during which the gas remains in the discharge (calculated based on the dimensions of the inter-dielectric space and the continuous N_2 gas flow rate), and *Duty Cycle* is the ratio between the plasma-on time and the liquid injection time. At zero continuous gas flow, the residence time of the precursor seems infinite. However, since the pressure in the chamber is maintained at 750 Torr by pumping, the liquid precursor flows inside the plasma chamber. Looking at Figure 6a, the thickness of the film obtained for a N_2 gas flow rate of 0.1 L.min^{-1} is comparable to the one of the films obtained in the absence of a continuous N_2 gas flow. If the average thickness of the deposit depends mainly on the residence time of the species in the discharge, it may be hypothesized that the pumping system generates a flow equivalent to ~0.1 L.min^{-1} continuous gas flow.

To assess the effect of the energy parameter provided by Equation (1) on the kinetics driving organosilicon thin-film deposition by direct liquid injection into nitrogen DBDs, the thickness profile extracted from Si-O-Si peak area as a function of energy was plotted for a total process duration of 4 min. As shown in Figure 8, the thickness of the deposited film, linked to the deposition rate, increases linearly with the energy in the early stages. Hence, the deposition rate is limited by the amount of energy provided to precursor

molecules, and not by precursor insufficiency [16,17,54]. However, beyond ~0.05 J.cm^{-2}, the increase becomes less significant with a departure from the proportional curve, which suggests either a saturation in conversion or a limitation in the precursor quantity; we will come back to this point later on.

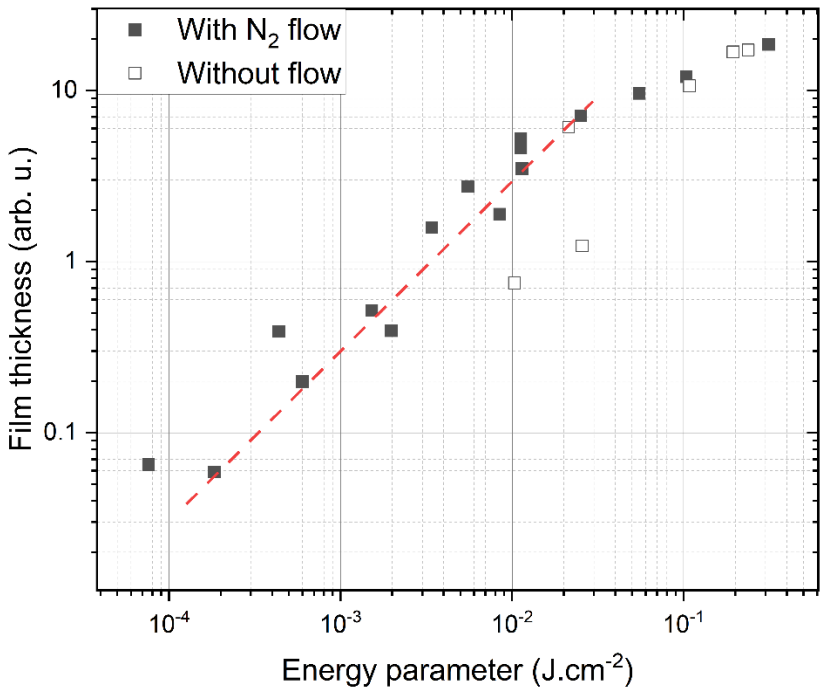

Figure 8: Variation of film thickness recorded for a total process time of 4 min. (linked to the deposition rate) as a function of the energy parameter. Pulsed injection time of 10 ms, pulsed injection frequency of 0.1 Hz. The results are shown for various plasma-on times and delay times between precursor injection and plasma ignition with or without a continuous N_2 gas flow.

5.5. Influence of the quantity of liquid injected into the discharge

In the previous sub-section, we have shown that the thickness of the deposited organosilicon film depends only on the plasma-on time and not on the delay between pulsed liquid injection and discharge ignition. Furthermore, by plotting the variation of film thicknesses as a function of the energy parameter, we have seen that the plasma deposition rate is first energy-limited and then deviates from this trend at higher energies. To examine the effect of the quantity of liquid injected into the discharge on the amount of plasma-deposited material, the liquid opening time of the direct-liquid injector (time during which the liquid flows from the liquid chamber of the injector to the injection chamber) was varied. Of note, all results presented previously were recorded at 5 ms liquid opening time and 10 ms injection duration. Figure 9a and b show the variation of liquid flow, film thickness, and mean power density injected into the DBD, respectively, as a function of liquid opening time (t_{liq}) between 2 and 6 ms, at constant injection duration (10 ms) and frequency (0.1 Hz). As expected, the results presented in Figure 9a reveal that the amount of liquid injected into the DBD cell increases linearly with t_{liq}. Such feature is linked to an increase in the number and/or size of the HMDSO droplets. Over the same range of experimental conditions, the power density injected into the DBD remains almost constant at around 0.2 $W.cm^{-2}$ (Figure 9c). As for the film thickness, also shown in Figure 9b, despite the significant rise in liquid flow, it does not increase with t_{liq}. As previously discussed from the data presented in Figure 8, this confirms that the discharge is saturated with precursor. In other words, the power provided by the discharge enables the deposition of the same quantity of precursor, irrespective of the amount of precursor injected. Here, in addition to plasma deposition and plasma polymerization, the energy is also used to

induce droplet charging, electrostatic deformation, and Coulomb fission. As for the departure from the linear trend observed at high energy parameters in Figure 8, since it cannot be linked to a precursor insufficiency, other mechanisms must be involved, for example, the gas phase coalescence of droplets because of mutual interactions [43,55] or different plasma polymerization processes.

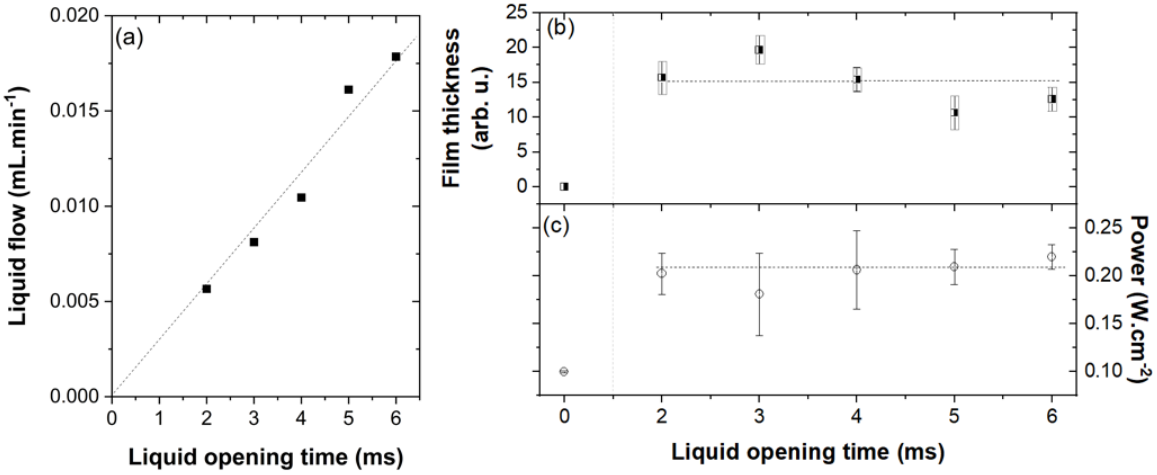

Figure 9: Variation of (a) liquid flow, (b) film thickness recorded for a total process time of 4 min. (linked to the deposition rate), and (c) mean power density injected into the DBD as a function of liquid opening time.

6. Conclusion

This study investigates the kinetics driving the plasma-assisted deposition of organosilicon thin films using pulsed HMDSO aerosols with nitrogen into a DBD at atmospheric pressure. The effects of plasma-on time, delay between precursor injection and plasma ignition, continuous gas flow, and liquid quantity on the thickness (or rate) of

the plasma-deposited film were assessed. The obtained results show that the deposit thickness (or rate) is proportional to the plasma-on time; however, it is independent of the plasma delay time. This indicates that the precursor is always present in the inter-dielectric gap, even if injection only occurs over a short time scale with respect to the pulsed injection frequency. In such conditions, thin-film deposition results from droplets charging and their transport towards the dielectrics by the low-frequency electric field. Moreover, the use of a nitrogen carrier gas flow leads to thinner films whose maximum thickness is shifted towards the exit of the substrate. Hence, the transport of droplets with the nitrogen carrier gas flow along the gas flow lines competes with the thin-film deposition as a result of plasma-droplet interactions on the substrate surface. Finally, the deposition is favored by an increase in the energy provided per precursor molecule. In addition to plasma deposition and polymerization, such energy is also used for droplet charging, electrostatic deformation, and fission. Future studies will aim at exploring the physico-chemical structure of such films, in particular the extent of plasma polymerization and retention of the initial monomer structure for technological applications.

7. Acknowledgments

The authors would like to thank Michel Féron for his contribution to this work and Mariam Rachidi for manuscript revisions. This work was financially supported by the Université Toulouse III - Paul-Sabatier and Direction des Relations Internationales of the Université de Montréal through their contributions to the Québec-France International Research Network on Nanomatériaux Multifonctionnels Contrôlés (IRN-NMC).

8. Data availability statement

The data are available from the corresponding author upon request.

References

[1] Massines F, Sarra-Bournet C, Fanelli F, Naudé N and Gherardi N 2012 Atmospheric pressure low temperature direct plasma technology: Status and challenges for thin film deposition *Plasma Processes and Polymers* **9** 1041–73

[2] Merche D, Vandencasteele N and Reniers F 2012 Atmospheric plasmas for thin film deposition: A critical review *Thin Solid Films* **520** 4219–36

[3] Vautrin-Ul C, Boisse-Laporte C, Benissad N, Chausse A, Leprince P and Messina R 2000 Plasma-polymerized coatings using HMDSO precursor for iron protection *Prog Org Coat* **38** 9–15

[4] Saloum S Ã, Naddaf M and Alkhaled B 2008 Properties of thin films deposited from HMDSO / O 2 induced remote plasma : Effect of oxygen fraction **82** 742–7

[5] Profili J, Levasseur O, Koronai A, Stafford L and Gherardi N 2017 Deposition of nanocomposite coatings on wood using cold discharges at atmospheric pressure *Surf Coat Technol* **309** 729–37

[6] Gherardi N, Maechler L, Naudé N and Massines F 2009 APGD and APTD for the deposition of silicon based thin films from N 2 O / HMDSO mixtures : application to gas-barrier layers *Ispc 19* pp 1–4

[7] Fanelli F 2010 Thin film deposition and surface modification with atmospheric pressure dielectric barrier discharges *Surf Coat Technol* **205** 1536–43

[8] Meunier L, Profili J, Babaei S, Asadollahi S, Sarkissian A, Dorris A, Beck S, Naudé N and Stafford L 2020 Modification of microfibrillated cellulosic foams in a dielectric barrier discharge at atmospheric pressure *Plasma Processes and Polymers* **2000158**

[9] Kale K H and Palaskar S 2010 Atmospheric pressure plasma polymerization of hexamethyldisiloxane for imparting water repellency to cotton fabric *Textile Research Journal* **81** 608–20

[10] Frari D Del, Bour J, Bardon J, Buchheit O, Arnoult C and Ruch D 2009 Hybrid Layers Deposited by an Atmospheric Pressure Plasma Process for Corrosion Protection of Galvanized Steel **9** 1–9

[11] Asadollahi S, Farzaneh M and Stafford L 2019 On the Icephobic Behavior of Organosilicon-Based Surface Structures Developed Through Atmospheric Pressure Plasma Deposition in Nitrogen Plasma *Coatings* **9** 679

[12] Lin Y-C and Wang M-J 2019 Fabrication of hydrophobic/hydrophilic HMDSO films by atmospheric pressure plasma jet deposition *Jpn J Appl Phys* **58** SAAC01

[13] Meshkova A S, Elam F M, Starostin S A, van de Sanden M C M and de Vries H W 2018 The role of carrier gas flow in roll-to-roll AP-PECVD synthesized silica moisture barrier films *Surf Coat Technol* **339** 20–6

[14] Lin Y and Yasuda' H 1995 Effect of Plasma Polymer Deposition Methods on Copper Corrosion Protection *J Appl Polym Sci* **60**

[15] Park S Y, Kim N, Kim U Y, Hong S I and Sasabe H 1990 Plasma Polymerization of Hexamethyldisilazane *Polym J* **22** 242–9

[16] Petersen J, Bardon J, Dinia A, Ruch D and Gherardi N 2012 Organosilicon Coatings Deposited in Atmospheric Pressure Townsend Discharge for Gas Barrier Purpose: Effect of Substrate Temperature on Structure and Properties *ACS Appl Mater Interfaces* **4** 5872–82

[17] Bardon J, Dieden R, Grysan P, Mertz G, Martin A, Delmée M and Ruch D 2019 Mechanical properties of thin plasma polymer coatings from hexanediol dimethacrylate and relations with their chemical properties *Surf Coat Technol* **358** 320–30

[18] Moreno-Couranjou M, Guillot J, Audinot J-N, Bour J, Prouvé E, Durrieu M-C, Choquet P and Detrembleur C 2020 Atmospheric pulsed plasma copolymerization of acrylic monomers_ Kinetics, chemistry, and applications *Plasma Processes and Polymers* **17**

[19] Manakhov A, Moreno-Couranjou M, Boscher N D, Rogé V, Choquet P and Pireaux J-J 2012 Atmospheric Pressure Pulsed Plasma Copolymerisation of Maleic Anhydride and Vinyltrimethoxysilane: Influence of Electrical Parameters on Chemistry, Morphology and Deposition Rate of the Coatings *Plasma Processes and Polymers* **9** 435–45

[20] Hilt F, Duday D, Gherardi N, Frache G, Didierjean J and Choquet P 2015 Plasma polymerisation of an allyl organophosphate monomer by atmospheric pressure pulsed-PECVD: insights into the growth mechanisms *RSC Adv* **5** 4277–85

[21] Starostin S A, Premkumar P A, Creatore M, van Veldhuizen E M, de Vries H, Paffen R M J and van de Sanden M C M 2009 On the formation mechanisms of the diffuse atmospheric pressure dielectric barrier discharge in CVD processes of thin silica-like films *Plasma Sources Sci Technol* **18**

[22] Raballand V, Benedikt J, Hoffmann S, Zimmermann M and von Keudell A 2009 Deposition of silicon dioxide films using an atmospheric pressure microplasma jet *J Appl Phys* **105** 083304

[23] Levasseur O, Stafford L, Gherardi N, Naudé N, Beche E, Esvan J, Blanchet P, Riedl B and Sarkissian A 2013 Role of substrate outgassing on the formation dynamics of either hydrophilic or hydrophobic wood surfaces in atmospheric-pressure, organosilicon plasmas *Surf Coat Technol* **234** 42–7

[24] Palumbo F, lo Porto C, Fracassi F and Favia P 2020 Recent Advancements in the Use of Aerosol-Assisted Atmospheric Pressure Plasma Deposition *coatings* **10**

[25] Mitev D, Radeva E, Peshev D, Cook M and Peeva L 2016 PECVD polymerised coatings on thermo-sensitive plastic support *Journal of Physics: Conference Series* vol 682 (Institute of Physics Publishing)

[26] O'Neill L, Herbert P A F, Stallard C and Dowling D P 2010 Investigation of the effects of gas versus liquid deposition in an aerosol-assisted corona deposition process *Plasma Processes and Polymers* **7** 43–50

[27] Coppins M 2010 Electrostatic Breakup in a Misty Plasma *Phys Rev Lett* **104** 065003

[28] Stancampiano A, Gallingani T, Gherardi M, Machala Z, Maguire P, Colombo V, Pouvesle J-M and Robert E 2019 Plasma and Aerosols: Challenges, Opportunities and Perspectives *Applied Sciences* **9** 3861

[29] Mejanes N de, Profili J, Babaei S, Naudé N and Stafford L 2021 Refined analysis of current–voltage characteristics in Townsend dielectric barrier discharges in nitrogen at atmospheric pressure *J Phys D Appl Phys* **54** 095204

[30] Profili J, Levasseur O, Naudé N, Chaneac C, Stafford L and Gherardi N 2016 Influence of the voltage waveform during nanocomposite layer deposition by aerosol-assisted atmospheric pressure Townsend discharge *J Appl Phys* **120** 053302

[31] Babaei S, Profili J, Asadollahi S, Sarkassian A, Dorris A, Beck S and Stafford L 2020 Analysis of transport phenomena during plasma deposition of hydrophobic coatings on porous cellulosic substrates in plane-to-plane dielectric barrier discharges at atmospheric pressure *Plasma Processes and Polymers* **17** 2000091

[32] Naudé N, Cambronne J-P, Gherardi N and Massines F 2005 Electrical model of an atmospheric pressure Townsend-like discharge (APTD) *The European Physical Journal Applied Physics* **29** 173–80

[33] Pipa A and Brandenburg R 2019 The Equivalent Circuit Approach for the Electrical Diagnostics of Dielectric Barrier Discharges: The Classical Theory and Recent Developments *Atoms* **7** 14

[34] Naudé N, Cambronne J-P, Gherardi N and Massines F 2005 Electrical model and analysis of the transition from an atmospheric pressure Townsend discharge to a filamentary discharge *J Phys D Appl Phys* **38** 530–8

[35] Li K, Gabriel O and Meichsner J 2004 Fourier transform infrared spectroscopy study of molecular structure formation in thin films during hexamethyldisiloxane decomposition in low pressure rf discharge *J Phys D Appl Phys* **37** 588–94

[36] Babaei S, Profili J, Asadollahi S, Sarkassian A, Dorris A, Beck S and Stafford L 2020 Analysis of transport phenomena during plasma deposition of hydrophobic coatings on porous cellulosic substrates in plane-to-plane dielectric barrier discharges at atmospheric pressure *Plasma Processes and Polymers* **17** 2000091

[37] Levasseur O, Stafford L, Gherardi N, Naudé N, Blanchard V, Blanchet P, Riedl B and Sarkissian A 2012 Deposition of Hydrophobic Functional Groups on Wood

Surfaces Using Atmospheric-Pressure Dielectric Barrier Discharge in Helium-Hexamethyldisiloxane Gas Mixtures *Plasma Processes and Polymers* **9** 1168–75

[38] Massines F, Gherardi N, Naudé N and Ségur P 2009 Recent advances in the understanding of homogeneous dielectric barrier discharges *The European Physical Journal Applied Physics* **47** 22805

[39] Cacot L, Carnide G, Kahn M L, Caquineau H, Clergereaux R, Naudé N and Stafford L 2022 Influence of pulsed gas injections on the stability of Townsend dielectric barrier discharges in nitrogen at atmospheric pressure *J Phys D Appl Phys*

[40] Gherardi N, Gouda G, Gat E, Ricard A and Massines F 2000 Transition from glow silent discharge to micro-discharges in nitrogen gas *Plasma Sources Sci Technol* **9** 340–6

[41] Tyl C, Lin X, Bouzidi M C, Dap S, Caquineau H, Ségur P, Gherardi N and Naudé N 2018 Investigation of memory effect in atmospheric pressure dielectric barrier discharge in nitrogen with small oxygen or nitric oxide addition *J Phys D Appl Phys* **51**

[42] Lin X, Tyl C, Naudé N, Gherardi N, Popov N A and Dap S 2020 The role of associative ionization reactions in the memory effect of atmospheric pressure Townsend discharges in N2 with a small O2 addition *J Phys D Appl Phys* **53** 205201

[43] Iqbal M M and Turner M M 2015 Investigations of Droplet-Plasma Interaction using Multi-Dimensional Coupled Model *Contributions to Plasma Physics* **55** 627–42

[44] Bennet E D, Mahony C M O, Potts H E, Everest P, Rutherford D, Askari S, McDowell D A, Mariotti D, Kelsey C, Perez-Martin F, Hamilton N, Maguire P and

Diver D A 2016 Precision charging of microparticles in plasma via the Rayleigh instability for evaporating charged liquid droplets *J Aerosol Sci* **100** 53–60

[45] Profili J, Dap S, Levasseur O, Naude N, Belinger A, Stafford L and Gherardi N 2017 Interaction of atomized colloid with an ac electric field in a dielectric barrier discharge reactor used for deposition of nanocomposite coatings *J Phys D Appl Phys* **50** 075201

[46] Bour J, Bardon J, Aubriet H, Frari D del, Verheyde B, Dams R, Vangeneugden D and Ruch D 2008 Different Ways to Plasma-Polymerize HMDSO in DBD Configuration at Atmospheric Pressure for Corrosion Protection *Plasma Processes and Polymers* **5** 788–96

[47] Enache I, Caquineau H, Gherardi N, Paulmier T, Maechler L and Massines F 2007 Transport Phenomena in an Atmospheric-Pressure Townsend Discharge Fed by N2/N2O/HMDSO Mixtures *Plasma Processes and Polymers* **4** 806–14

[48] Sarra-Bournet C, Gherardi N, Turgeon S, Laroche G and Massines F 2009 Deposition of functional hydrogenated amorphous carbon-nitride film (a-CN : H) using C 2 H 4 / N 2 townsend dielectric barrier *The European Physical Journal Applied Physics* **22820** 1–6

[49] Coppins M 2004 The critical droplet size in a misty plasma *31st EPS Conference on Plasma Phys. Lindon*

[50] Maguire P D, Mahony C M O, Kelsey C P, Bingham A J, Montgomery E P, Bennet E D, Potts H E, Rutherford D C E, McDowell D A, Diver D A and Mariotti D 2015 Controlled microdroplet transport in an atmospheric pressure microplasma *Appl Phys Lett* **106** 224101

[51] Li K-Y, Tu H and Ray A K 2005 Charge Limits on Droplets during Evaporation *Langmuir* **21** 3786–94

[52] Rayleigh, Lord 1882 XX. *On the equilibrium of liquid conducting masses charged with electricity The London, Edinburgh, and Dublin Philosophical Magazine and Journal of Science* **14** 184–6

[53] Hegemann D, Bülbül E, Hanselmann B, Schütz U, Amberg M and Gaiser S 2021 Plasma polymerization of hexamethyldisiloxane: Revisited *Plasma Processes and Polymers* **18** 2000176

[54] Shelemin A, Choukourov A, Kousal J, Slavínská D and Biederman H 2014 Nitrogen-doped TiO2 nanoparticles and their composites with plasma polymer as deposited by atmospheric pressure DBD *Steel Res Int* **11** 864–77

[55] Turner M M, Iqbal M M and Turner M M 2013 Behaviour of HMDSO Liquid Precursor Droplets in Atmospheric Pressure Discharge Plasma and Gas Mixture